Effect of Rapid Mold Surface Inducting Heating on the Replication Ability of Microinjection Molding Light-Guided Plates with V-grooved Microfeatures

Ming-Shyan Huang, Jyh-Cheng Yu, Ying-Zhi Lin

Department of Mechanical and Automation Engineering, National Kaohsiung First University of Science and Technology, Nanzih District, Kaohsiung City, 811 Taiwan, Republic of China

Received 30 January 2010; accepted 2 May 2010
DOI 10.1002/app.32735
Published online 1 July 2010 in Wiley InterScience (www.interscience.wiley.com).

ABSTRACT: This study applies a magnetic induction heating method for rapid and uniform heating of a mold surface for injection molding of 2-inch light-guided plates (LGPs). Mold temperature is an important process parameter that affects microinjection molding quality. This research investigates the effects of high-mold surface temperature generated by induction heating in enhancing the replication rate of microfeatures of LGPs. This study has three stages. First, an appropriate power rate setting is determined for induction heating and injection molding process window. Second, all key parameters affecting microfeature quality are identified to determine the optimum LGP micromolding parameters using the Taguchi and ANOVA methods. Third, the quality of microfeature heights and angles are experimentally verified. Polymethyl methacrylate was molded under various injection molding conditions to replicate an electroformed nickel stamper with V-grooves 10 μm in width and 5 μm in depth. In this investigation, injection speed was set in the conventional range. Experimental findings indicate that instead of high-mold temperature, the combination of low mold temperature and high surface temperature obtained using induction heating improve replication quality and reduce cycle time. © 2010 Wiley Periodicals, Inc. J Appl Polym Sci 118: 3058–3065, 2010

Key words: induction heating; light-guided plates; microinjection molding; rapid surface heating

INTRODUCTION

Microinjection molding has garnered increased attention in industry and academia due to its promising advantages of low cost and suitability for mass production.[1–3] One of the primary applications of microinjection molding is to light-guided plates (LGPs). Notably, LGPs are an important component of a back-lighted unit that determines optical efficiency and is mainly used to guide scattered rays to improve panel brightness uniformity. Nevertheless, whether a ray travels in the desired direction depends on the replication effect of microfeatures on the LGP surface during injection molding. Injection molding LGPs with microfeatures that have a high aspect ratio and micrometer-scale width usually has a low replication rate.[4,5] Several studies suggested that mold temperature is the predominant factor affecting micromolding and that high-mold temperature promotes feature transfer during micromolding.[6–8] A high-mold temperature, higher than the glass transition temperature of processed plastics, may reduce the number of defective finished products and increases the likelihood of completely filling microfeatures.[9–11] However, maintaining mold temperature above the glass transition temperature or crystallization temperature during the filling stage and then lowering mold temperature to below the heat deflection temperature during the packing and cooling stages is difficult without increasing cycle time and, thereby, production cost.

To achieve a high-mold temperature without increasing cycle time, numerous studies have attempted to heat only the mold surface.[12] These studies have used infrared thermal radiation heating, frame heating, external hot air heating, induction heating, proximity heating, and coating heating.[13–18] In this study, an induction heating system is employed to provide the high-mold temperature required for the short filling stage during replication of LGP microfeatures, and to rapidly reduce mold temperature during cooling to reduce cooling time for the molded parts. The principle of induction heating heats metals by electromagnetic induction with its skin effect, by which heat transfer occurs only on the surface of the mold cavity that is heated

Correspondence to: M.-S. Huang (mshuang@ccms.nkfust.edu.tw).

Contract grant sponsor: National Science Council of the Republic of China; contract grant number: NSC98-2221-E-327-011.

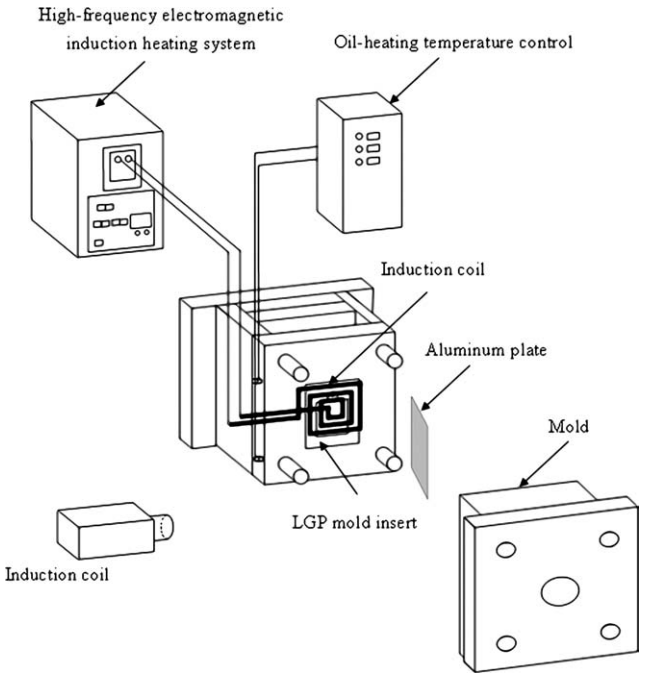

Figure 1 Experimental setup for rapid induction heating of a 2-inch LGP mold surface.

by an induction coil. Accordingly, heat absorption efficiency of the cavity surface is high and surface heat dissipates rapidly. Furthermore, power, heating distance, and coil design directly govern heat transfer efficiency.[19] As induction heating is noncontact heating, it does not alter mold structure. As heating coils can be replaced on the basis of the shape or depth of a cavity, induction heating can be used to heat-complex mold surfaces.

This investigation uses a 2-inch LGP injection mold with V-grooved microfeatures 10-μm wide and 5-μm deep to verify the replication of microfeatures by induction heating. The study has three stages: (1) to select the most appropriate power rate setting for induction heating and an injection molding process window, (2) to identify the key parameters affecting the microfeature quality and generates the optimum settings of LGP micromolding parameters using the Taguchi method and analysis of variance (ANOVA), and (3) to experimentally verify the quality of microfeature heights and angles.

INDUCTION HEATING SYSTEM

Figure 1 shows the configuration of the induction heating experiment for heating a 2-inch LGP mold surface. The high-frequency induction heating equipment in the experiment comprise a transistor-type high-frequency oscillator, a high-frequency output transformer with an input power of 25 kW and output oscillation frequency of 30–100 kHz, an induction coil, and a water cooling system. Figure 2 shows the geometry of an induction coil. Typical heating coils can be classified as single-turn and multiturn types. The former are appropriate for heating small areas, whereas the latter provide relatively higher power, require a shorter heating time and are for heating large areas. The heating coil used in this study is a three-layered turned copper wire for heating a small area. Coil shape and size, number of coil turns, and relative location of the coils affect performance in rapidly and uniformly heating a surface.[19] Traditional single-layered coils have a disadvantage in that they produce a nonuniform temperature distribution over the cross and depth sections of a heated target. The multilayered induction coil employed in this research can increase the efficiency of mold-surface heating and the uniformity of the temperature obtained.

Induction heating heats a metal by electromagnetic induction. According to Faraday's law and Lenz's law, passing alternating current through heating coils produces an alternating magnetic field that can be used to heat an object. When processed magnetic or nonmagnetic conductive workpieces are placed in the alternating magnetic field established by the heating coils, workpiece resistance and flow of eddy currents (I_c) therein generate a heating power of I_c^2R. Factors dominating an induction heating system are current frequency and heating coil shape. Current frequency affects penetration depth. A current frequency can be selected on the basis of material properties of resistance and magnetic permeability. A high frequency typically corresponds to shallow heat penetration.

LGP MOLD INSERT

The molded part is a flat LGP 40 mm long, 30 mm wide, and 1 mm thick (Fig. 3). The microfeatures are V-grooves 10 μm wide and 5 μm deep. This single cavity mold is designed with a fan-shaped gate 8 mm wide and 0.7 mm thick. The cooling system has two inlets and two outlets (Fig. 4). A FANUC α-30i all electrical injection molding machine is used for

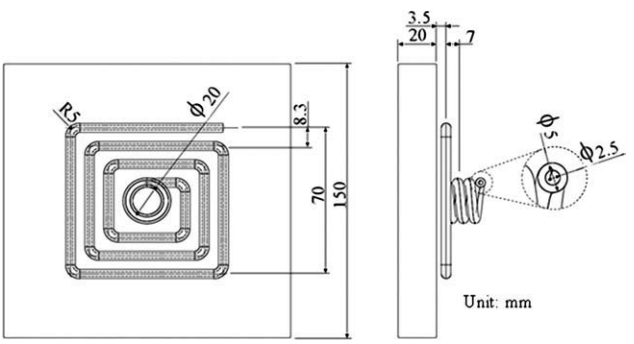

Figure 2 The geometry and dimensions an induction coil.

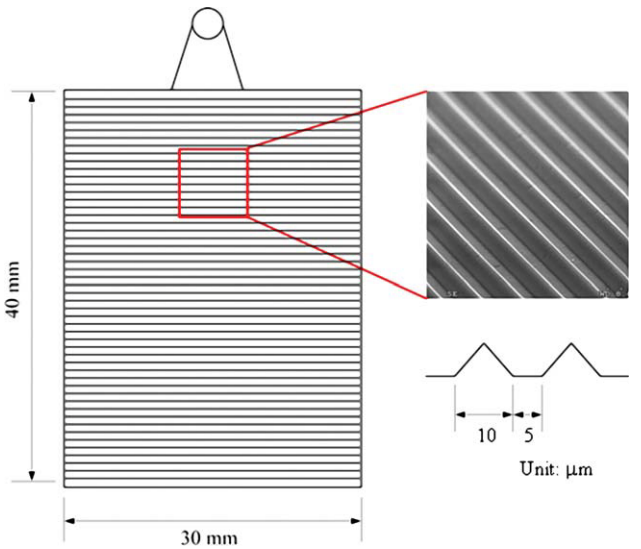

Figure 3 The microfeature of a 2-inch LGP mold insert. [Color figure can be viewed in the online issue, which is available at www.interscience.wiley.com.]

precise molding. The plastic used in this experiment was Polymethyl methacrylate (Kurarary GH-1000S) with a glass transition temperature of 104°C). In the experiment, a thermometer and infrared ray thermal imaging system (ThermoVision A20M; Precision: within 100±2°C; above 100±2°C of a reading) are used to measure temperature and record variations in mold temperature due to induction heating. Thus, thermal images are captured to elucidate further the effect of induction heating current, frequency, and duration on the mold surface. Figure 5 shows the positions on the mold surface where temperature was measured.

Under each molding condition, two LGPs are sampled. After cooling the samples for 24 h, the microfeatures of the LGP are measured using a surface profiler (KLA-Tencor alpha-step surface profile detector).

TAGUCHI PARAMETERS

The Taguchi method utilizes the signal to noise (*S/N*) ratio approach to measure deviation in quality from the desired value. The *S/N* ratio instead of the average value is also used to convert experimental results into a value for the evaluation characteristic in optimum parameter analysis. The unit of the *S/N* ratio is dB and can be defined as

$$\eta = -10\log(MSD), \tag{1}$$

where *MSD* is the mean-squared deviation for the output characteristic. The *S/N* ratio characteristics can be divided into three types—nominal is better, smaller is better, and larger is better—when quality characteristics are continuous for engineering analysis. As the study objectives are to identify the optimum setting that minimizes replication errors in height and angle of LGP microfeatures, the smaller is better quality characteristic is employed. The *MSD* for the smaller-the-better quality characteristic can be expressed as

$$MSD = \frac{1}{M \times n}\sum_{j=1}^{m}\sum_{i=1}^{n}\Delta Y_{ij}^2, \tag{2}$$

where ΔY_{ij} is the difference between the measured value and target value for the *i*th sample and the *j*th

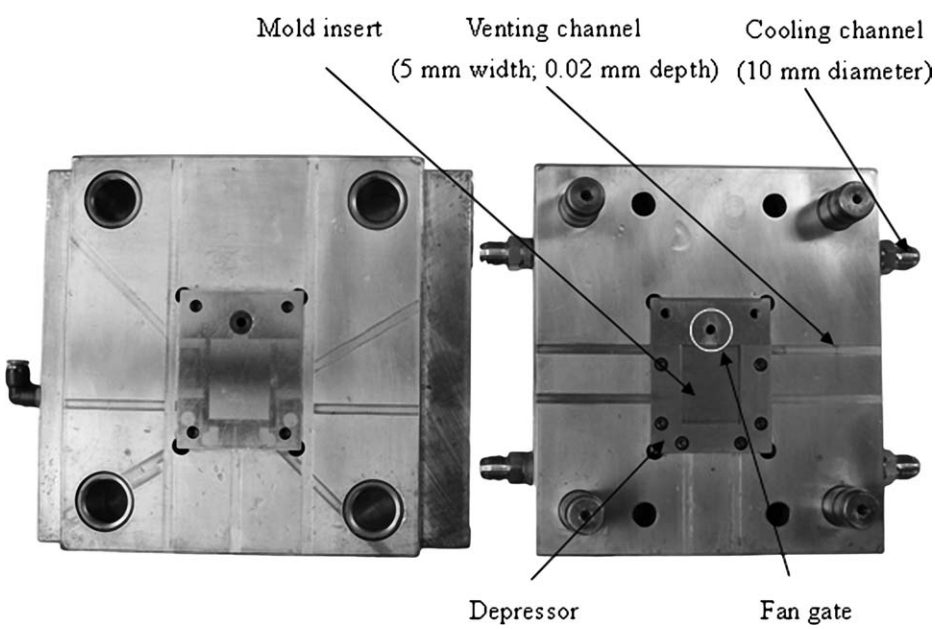

Figure 4 The geometry of a 2-inch LGP injection mold.

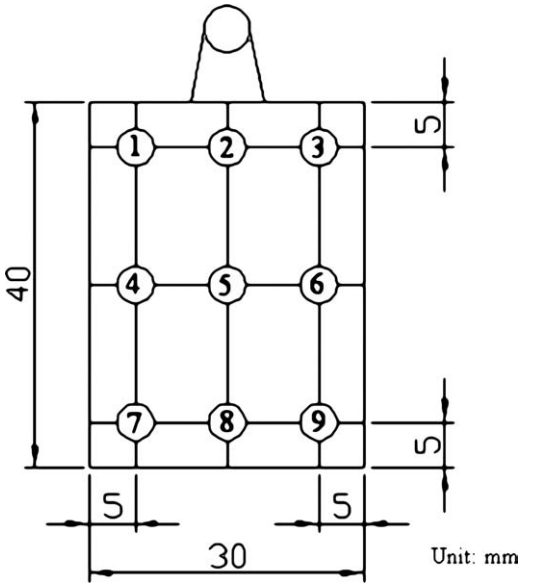

Figure 5 The measured locations of mold-surface temperature on a 2-inch LGP mold insert.

measurement point, and m and n represent the total number of samples and total measurement points in one sample, respectively. Because $-\log$ is a monotone decreasing function, the *S/N* value should be maximized. Thus, the *S/N* values are calculated by Eqs. (1) and (2). Errors in replicated height and angle on the LGP under process parameters of injection speed, packing pressure, mold temperature, cooling time, and mold-surface temperature are analyzed with the L_{18} orthogonal array of the Taguchi method and their *S/N* ratios.

The experiments are executed according to L_{18} orthogonal array. Table I lists the control factors and levels of the Taguchi experiments. In this study, six control factors are chosen, namely, injection speed, packing pressure, packing time, mold temperature, cooling rate, and mold-surface temperature. According to the short-shot experiment conducted and specification limits of the employed machine, the following ranges of control factors were selected: injection speed (*A*, 180–200 mm/s); packing pressure (*B*, the first stage pressure at 50–70 MPa; the second stage pressure at 40 MPa); packing time (*C*, 4–8 s); mold temperature (*D*, 60–80°C); cooling time (*E*, 30–40 s); and mold-surface temperature (*F*, 110–150°C). Each of the six molding factors is designed with three levels due to possible nonlinear factor effects.

TABLE I
The Control Factors and Levels of the Taguchi Experiments

	Level		
Control factor	1	2	3
A. Injection speed (mm/s)	180	190	200
B. Packing pressure (MPa)	50/40	60/40	70/40
C. Packing time (s)	4–5	6–5	8–5
D. Mold temperature (°C)	60	70	80
E. Cooling rate (s)	30	35	40
F. Mold-surface temperature (°C)	110	130	150

To determine the optimum setting for the power rate in the induction heating system, this study examines the temperature profiles of a heated Ni plate that is the mold insert in the 2-inch LGP; these temperature profiles correspond to various power rates. Figure 6 shows the mold temperature profiles at p2 after induction heating at power rates of 25, 30, 35, and 40%. The temperature profile attains its maximum value at 3 sec—the time at which the induction coil in the experiment is removed. The power rate of 40% generates the highest heating temperature and lowest cooling rate among the four temperature profiles, i.e., the temperature drops instantly from 350 to 280°C between 3 and 4 s. This 70°C difference at a 40% power rate is significantly higher than 31°C at a power rate of 35%, 24°C at a power rate of 30%, and 28°C at a power rate of 25% and, thus, is undesirable in terms of performance on gaining a constant temperature, and reducing energy consumption. Although the temperature variation at a power rate of 25% is relatively low, it remains impractical due to a slow heating rate, which increases cycling time. The best performance among these four power rates for mold-surface heating is attained at power rates of 30 and 35%, which achieve two similar temperature profiles. To further consider the issue of power consumption, the 30% power rate is thus selected for the LGP microinjection molding experiment.

TAGUCHI EXPERIMENTAL RESULTS AND ANOVA ANALYSIS

The ANOVA method was utilized to establish the relative significance of all factors.[20] Based on

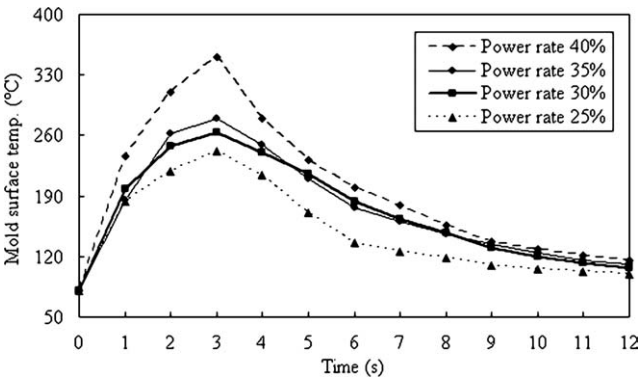

Figure 6 Mold temperature profiles at the p2 measurement location with induction heating at power rates of 25, 30, 35, and 40%.

TABLE II
The L_{18} Orthogonal Array and Experimental Results

Exp. No.	Injection speed (mm/s)	Packing pressure (MPa)	Packing time (s)	Mold temp. (°C)	Cooling time (s)	Mold-surface temp. (°C)	Heights (μm) Average	S/N	Angle (°) average	S/N
1	180	70/40	8/5	70	35	110	0.65	3.68	5.07	−14.12
2	180	60/40	6/5	60	30	150	0.55	5.27	1.99	−5.98
3	180	50/40	4/5	80	40	130	0.48	6.46	2.73	−8.80
4	190	70/40	8/5	80	40	150	0.45	6.88	0.93	0.33
5	190	60/40	6/5	70	35	130	0.54	5.24	2.52	−8.65
6	190	50/40	4/5	60	30	110	2.25	−7.03	19.77	−25.92
7	200	70/40	6/5	80	30	130	0.47	6.56	1.73	−5.27
8	200	60/40	4/5	70	40	110	1.88	−5.49	13.83	−22.81
9	200	50/40	8/5	60	35	150	0.51	5.88	1.55	−3.85
10	180	70/40	6/5	60	40	110	1.06	−0.50	8.08	−18.15
11	180	60/40	4/5	80	35	150	0.48	6.43	2.33	−7.40
12	180	50/40	8/5	70	30	130	0.49	6.15	1.89	−5.54
13	190	70/40	4/5	60	35	130	0.64	3.92	4.52	−13.10
14	190	60/40	8/5	80	30	110	1.07	−0.55	5.34	−14.57
15	190	50/40	6/5	70	40	150	0.53	5.51	2.14	−6.64
16	200	70/40	4/5	70	30	150	0.55	5.19	1.09	−0.87
17	200	60/40	8/5	60	40	130	1.12	−0.98	7.56	−17.59
18	200	50/40	6/5	80	35	110	2.60	−8.29	22.19	−26.92
Optim. Combin.	180	70/40	8/5	70	30	150	0.45	7.06	0.93	0.38

experimental results obtained with the L_{18} orthogonal array (Table II), ANOVA shows the relative influences of factors and interactions assigned to an orthogonal array. Table III shows the ANOVA results after pooling the effects at a 95% confidence level.

From the ANOVA table, the effects of injection molding factors on the final quality of LGP microfeatures were determined. The mold-surface temperature and injection speed significantly impact the replication height and the angles of V-grooved microfeatures. According to the optimum condition of "smaller is better," the levels of factors contributing to the smallest error in height are preferred. From the *S/N* response chart (Table IV), the smallest replication error for height was attained with an injection speed of 180 mm/s, packing pressure of 70 MPa, packing time of 8 s, mold temperature of 70°C, cooling time of 35 s, and mold-surface temperature of 150°C. Furthermore, the smallest replication error for angles was attained at an injection speed of 180 mm/s, packing pressure of 70 MPa, packing time of 8 s, mold temperature of 70°C, cooling time of 30 s, and mold-surface temperature of 150°C. These two sets of optimum parameters are the same and can be selected as the optimum process parameters excluding the insignificant factor of cooling time. As terms of a short cycle time, a cooling time of 30 s (instead of 35 s) is selected as an optimum parameter to ensure height and angle quality.

TABLE III
The ANOVA Results

Error of height				
Source of variation	DOF	Sum of squares	Variation	*F*
Injection speed	2	50.69	25.34	4.67
Packing pressure	2	30.12	15.06	2.78
Packing time	2	11.41		
Mold temperature	2	17.51	8.75	1.61
Cooling time	2	2.23		
Mold-surface temperature	2	276.65	138.33	25.51
Pooled error	13	70.48	5.42	
Total	17	427.94		
Error of angle				
Injection speed	2	24.99		
Packing pressure	2	76.03	38.02	4.35
Packing time	2	48.51	24.25	2.77
Mold temperature	2	65.09	32.55	3.72
Cooling time	2	27.43		
Mold-surface temperature	2	825.24	412.62	47.17
Pooled error	15	131.21	15.76	
Total	17	1146.08	8.75	

VERIFICATION EXPERIMENT

Additional verification was performed to assess the effectiveness of the optimum process parameters identified with the Taguchi method. To illustrate the effect of induction heating on the mold surface, the optimum process parameters without introducing induction heating were further tested and compared. The two set points, the induction heating-assisted experiment and the oil heating-assisted experiment, were utilized to inject 50 molds as measurement samples. The process parameters of the induction heating-assisted experiment were injection speed of 180 mm/s, packing pressure of 70 MPa, packing time of 8 s, mold temperature of 70°C, cooling time

TABLE IV
The S/N Response Chart

Error of height						
Factor effect level	A Injection speed (mm/s)	B Packing pressure (MPa)	C Packing time (s)	D Mold temperature (°C)	E Cooling time (s)	F Mold surface temperature (°C)
1	4.58	4.29	3.51	2.91	1.98	5.86
2	2.33	1.65	2.30	3.38	2.81	4.56
3	0.48	1.45	1.58	1.09	2.60	−3.03
Difference	4.10	2.48	1.93	2.29	0.83	8.89
Rank	2	3	5	4	6	1
Optimum combination	180	70	8	70	35	150
Error of angle						
1	−13.01	−11.54	−12.23	−13.45	−15.29	−7.08
2	−14.44	−15.84	−14.95	−12.78	−15.35	−12.83
3	−15.90	−15.96	−16.16	−17.11	−12.70	−23.43
Difference	2.89	4.42	3.93	4.33	2.65	16.35
Rank	5	2	4	3	6	1
Optimum combination	180	70	8	70	30	150

of 30 s, and mold-surface temperature of 150°C. The process parameters of the oil heating-assisted experiment were injection speed of 180 mm/s, packing pressure of 70 MPa, packing time of 8 s, mold temperature of 70°C, and cooling time of 30 s.

Figure 7 shows the normal distribution of quality characteristics in terms of the probability density function. The solid lines in Figures 7(a,b) indicate the average height and angle distributions of LGP microfeatures in the oil heating-assisted experiment, respectively, whereas the solid lines in Figures 7(c,d) represent the average height and angle distributions of the induction heating-assisted experiment, respectively. In this case study, the oil heating-assisted experiment obtained LGP replication rates of only 60.5 and 69.4% for the average height and angle of nine-point microfeatures, respectively. Conversely, the performance of the induction heating-assisted

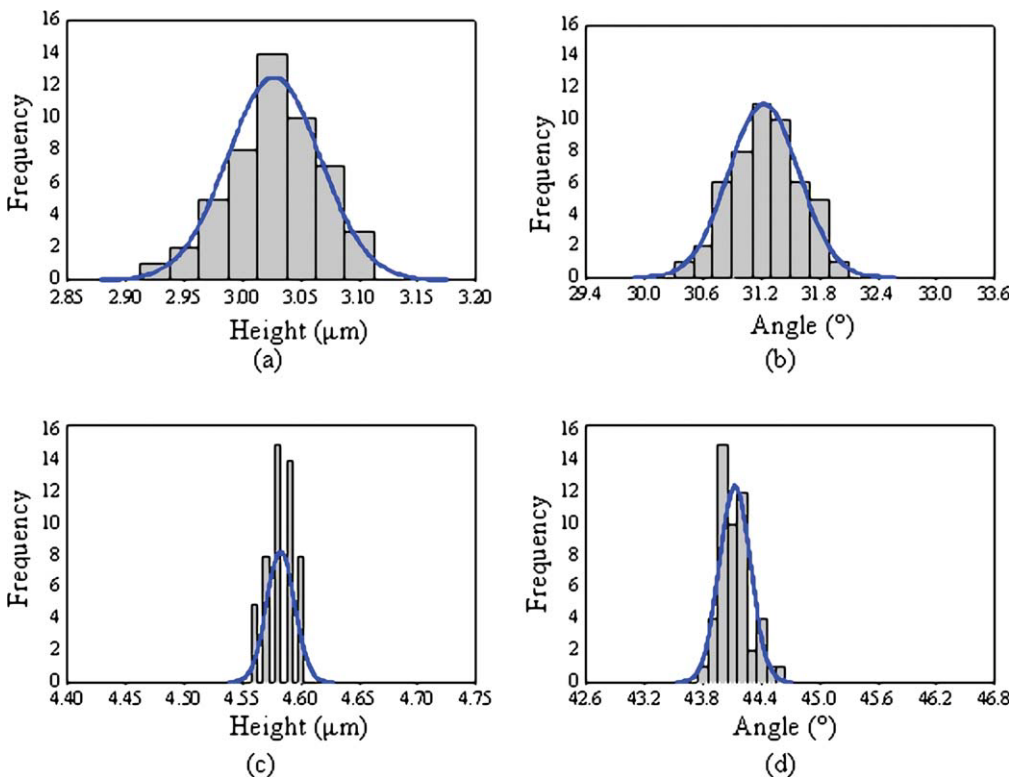

Figure 7 The average nine-point height and average nine-point angle distribution of LGP microfeatures: (a) height by the oil heating experiment; (b) angle by the oil heating experiment; (c) height by the induction-heating experiment; and (d) angle by the induction-heating experiment. [Color figure can be viewed in the online issue, which is available at www.interscience.wiley.com.]

TABLE V
Performance of the 2-Inch LGP Microinjection Molding with the Oil Heating-Assisted and Induction Heating-Assisted Experiments

	Oil heating-assisted		Induction heating-assisted	
	Average nine-point height (μm)	Average nine-point angle (°)	Average nine-point height (μm)	Average nine-point angle (°)
Average	3.03	31.22	4.58	44.13
Standard deviation	0.04	0.36	0.01	0.16

experiment generated LGP replications rates of 91.6 and 98.1% for the height and angle of nine-point microfeatures, respectively. Thus, the average value and standard deviation of part qualities (Table V) were markedly improved using the method.

Figure 8 shows the scanning electron microscope (SEM) micrographs of a 2-inch injection-molded LGP part. For example, the replication effect at point p5 (located at the middle of the molded part) on microfeatures is significantly improved by induction heating.

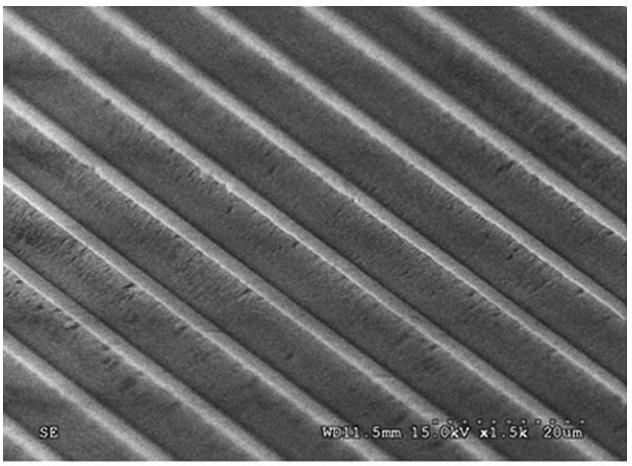

(a) 'p5' measuring location (induction heating)

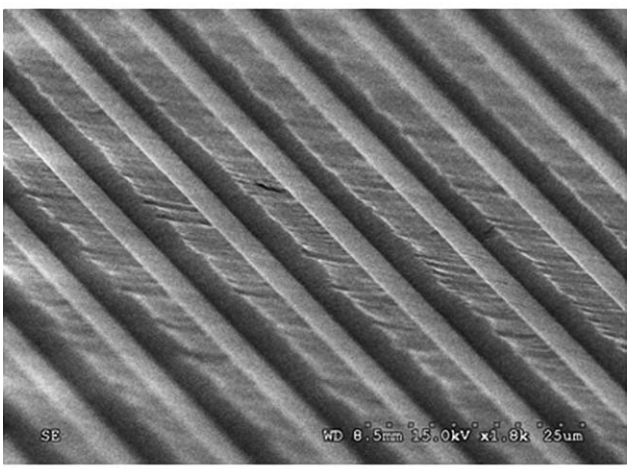

(b) 'p5' measuring location (without induction heating)

Figure 8 The SEM micrographs of 2-inch LGP microinjection molded parts.

CONCLUSIONS

This study investigates the effects of rapid mold-surface induction heating on the replication ability of microinjection molding LGPs with V-grooved microstructures within the conventional injection speed range. The following conclusions are drawn from study results.

(1). The optimum process parameters obtained with a Taguchi orthogonal array table and ANOVA correspond to an injection speed of 180 mm/s, packing pressure of 70 MPa, packing time of 8 s, mold temperature of 70°C, cooling time of 30 s, and mold-surface temperature of 150°C.
(2). The ANOVA result indicates that mold-surface temperature and injection speed are the most significant control parameters affecting the replication ability of microfeatures. Moreover, an increase in mold-surface temperature to 150°C increases the replication rate of average nine-point height of microfeatures to 91.6%, and that of average nine-point angle to 98.1%.
(3). Experimental results show that when mold-surface temperature reached a critical value of ~ 140°C, replication rate of the molded parts became significantly improved.

The authors appreciate Ted Knoy for his editorial assistance.

References

1. Wimberger-Friedl, R. J. Injection Molding Technol 2000, 4, 78.
2. Yao, D.; Kim, B. J Micromech Microeng 2002, 12, 604.
3. Wu, C. H.; Chen, W. S. Sensor Actuator Phys 2006, 125, 367.
4. Xu, G.; Yu, L.; Lee, J.; Koellingt, K. W. Polym Eng Sci 2005, 866.
5. Yokoi, H.; Han, X.; Takahashi, T.; Kim, W. K. Polym Eng Sci 2006, 1140.
6. Liou, A. C.; Chen, R. H. Int J Adv Manuf Technol 2006, 28, 1097.
7. Sha, B.; Dimov, S.; Griffiths, C.; Packianather, M. S. J Mater Process Technol 2007, 183, 284.
8. Yu, M. S.; Young, W. B.; Hsu, P. M. Mater Sci Eng A 2007, 460, 288.
9. Chen, S. C.; Chang, Y.; Chang, Y. P.; Chen, Y. C.; Tseng, C. Y. Int Commun Heat Mass Transfer 2010, 37, 517.

10. Song, M. C.; Liu, Z.; Wang, M. J.; Yu, T. M.; Zhao, D. Y. J Mater Process Technol 2007, 187, 668.
11. Chen, C. P.; Chuang, M. T.; Hsiao, Y. H.; Yang, Y. K.; Tsai, C. H. Expert Syst Appl 2009, 36, 10752.
12. Yao, D.; Chen, S. C.; Kim, B. H. Adv Polym Technol 2008, 207, 233.
13. Chang, P. C.; Hwang, S. J. J Appl Polym Sci 2006, 102, 3704.
14. Yim, S. J. U.S. Pat. 6,638,048 (2003).
15. Hendry, J. W. U.S. Pat. 4,201,742 (1980).
16. Huang, M. S.; Tai, N. S. J Appl Polym Sci 2009, 113, 1345.
17. Yao, D.; Kimerling, T. E.; Kim, B. Polym Eng Sci 2006, 46, 938.
18. Yao, D.; Kim, B. Appl Therm Eng 2003, 23, 341.
19. Huang, M. S.; Huang, Y. L. Int J Heat Mass Transf 2010, 53, 2414.
20. Iversen, G. R.; Norpoth, H. SAGE University Papers: California, 1976.